# Model High-Performance Adhesive Systems

JEREMY H. KLUG, JAMES C. SEFERIS

Polymeric Composites Laboratory, Department of Chemical Engineering, University of Washington, Box 351750, Seattle, Washington 98195-1750

*Received 7 March 1997; accepted 23 April 1997*

**ABSTRACT:** A study investigating the affect of formulating procedures on material properties was performed for model high-performance epoxy adhesives. Analyses were conducted on materials fabricated with 16 wt % butadiene–acrylonitrile reactive rubber, difunctional and tetrafunctional epoxies, bisphenol A, dicyandiamide, and diuron. Prereaction steps involving the reactive rubber, bisphenol A, and epoxies were varied so that different systems were obtained prior to and after cure. Lap shear and mode I and II fracture toughness tests showed that the formulating procedure significantly affected the performance properties. Differential scanning calorimetry revealed that the formulating procedure slightly affected the number of bonds formed during cure. Dynamic mechanical analysis suggested that increased flexibilized rubber in the continuous phase of the adhesives may lead to inferior bonding characteristics. This analysis also showed that the dispersed phase composition was largely unaffected by the formulating procedure and not dependent on the size or shape of the dispersed phase. Finally, optical microscopy showed that the formulating–mixing procedure had a strong influence on the size and shape of the dispersed phases. Overall, the results suggested that polymer mobilities and structure affected the morphology and adhesive ability and must be analyzed with fundamental processing–structure–property interrelationships. © 1997 John Wiley & Sons, Inc. J Appl Polym Sci **66:** 1953–1963, 1997

**Key words:** epoxy; adhesive; thermal analysis; morphology; fracture toughness

## INTRODUCTION

Epoxies have long been used in aerospace adhesive formulations because of their wide range of beneficial qualities. They are relatively inexpensive materials, bond and/or adhere well to a wide range of substrates, can be formulated to possess long pot lives, and are curable with many different hardeners.[1] Epoxies also are inherently less brittle than other commonly used aerospace matrix materials, such as phenolics and cyanate esters; however, certain applications still require improvements in the fracture toughness behavior. These improvements are often obtained by the addition of relatively low quantities of toughening agents.

Liquid reactive carboxyl terminated butadiene acrylonitrile (CTBN) elastomers have been employed in epoxies for several decades.[2–9] When combined with the host material prior to cure, a network containing CTBN dissolved or reacted in the matrix, as well as the formation of secondary rubber-rich dispersed phases, allows for orders of magnitude improvements in toughness characteristics. Extensive research has been conducted investigating CTBN behavior in such areas as optimum toughening particle size, toughening mechanisms, optimum adhesive layer thickness, bimodal particle distribution influence, secondary phase formation and growth, and much more.[2,3,6,7,10–15]

The analyses of different adhesive characteristics often involve utilizing model systems. Model

*Correspondence to:* J. C. Seferis.

Journal of Applied Polymer Science, Vol. 66, 1953–1963 (1997)
© 1997 John Wiley & Sons, Inc. CCC 0021-8995/97/101953-11

polymer systems provide the opportunity for obtaining a fundamental understanding of material's processing–structure–property interrelationships, which are essential for design and manufacturing purposes.[16] Model prepreg systems have been developed previously by Seferis and coworkers to investigate commercial prepreg materials.[17,18] The information generated in these studies has allowed for improvements in commercial systems through specialized teams created and composed of material suppliers, customers, manufacturers, and academia.[19] This current study is undertaken in an effort to transfer and extend this methodology to aerospace-grade adhesive materials.

As previously mentioned, much focus has been put on understanding the different phenomena that occur in toughened epoxy materials to yield the final morphology and properties. The previously mentioned studies have often dealt with varying cure conditions or chemical compositions. However, little attention has been given to differences in an adhesive material's morphology and properties due to the formulating procedure involving prereactions or formation of intermediate materials. The purpose of this investigation is to analyze how these formulating dependencies can affect the material's intermediate and final properties. With these slight changes in preparatory procedures, improved qualities may be obtained. This may allow for the optimization of performance for the adhesives both as bulk materials and in use with aerospace composite material.

## EXPERIMENTAL

The model adhesive resins analyzed in this study were prepared from a combination of epoxy materials. A difunctional epoxy, Epon® 828 (EEW = 190), and a tetrafunctional epoxy, Araldite® MY9512 (EEW = 107), were used in the synthesis of the adhesive resin systems. Butadiene–acrylonitrile liquid reactive rubber (Hycar® 1300 × 9 CTBN; 18 wt % acrylonitrile) was utilized as the toughening elastomeric material and bisphenol A as a chain extender for the epoxy resins. Dicyandiamide (10 $\mu$m average particle diameter) accelerated with diuron acted as the curing agent mixture. Triphenylphosphine (TPP), in the amount of approximately 0.2 wt %, was used to catalyze the epoxy–rubber and epoxy–bisphenol A (BPA) reactions. A summary of the base components and quantities used in all of the formulations is shown in Table I.

**Table I Base Materials and Quantities for Each Model Adhesive**

| Component | Quantity (wt %) |
|---|---|
| Difunctional epoxy | 57.3 |
| Tetrafunctional epoxy | 11.5 |
| Bisphenol A | 8.0 |
| Butadiene–acrylonitrile rubber | 15.4 |
| Dicyandiamide | 5.3 |
| Diuron | 2.2 |
| Triphenylphosphine | 0.3 |

Epoxy mixing, CTBN adduction, and BPA addition were performed in a well-stirred vessel at a temperature of 145°C. A period of one-half hour (each) was allowed for both of the prereactions: the CTBN adduction, or the BPA chain extension of the epoxy material in the formulations. After the prereactions were performed, the material was allowed to cool to 115°C, at which time the curing agent, accelerator, and epoxy mixture was added. A mixing time of approximately three minutes was allowed, after which the material was quenched to room temperature to avoid cure initiation.

Each of the resin formulations was filmed on an industrial size prepregging machine[20] using a hot plate temperature of 77°C. A spunbonded nonwoven polyester scrim material, Reemay® 2250, was also incorporated into the resin film for flow control to give a final adhesive thickness of 0.1 mm. The system was frequently checked, and no sign of resin starvation was seen in the final model adhesive products.

Thermal analyses were performed on the cured and uncured materials using differential scanning calorimetry (DSC) and dynamic mechanical analysis (DMA). TA Instrument 912 DSC and 983 DMA modules were utilized for the study, both interfaced to a Thermal Analyst 2000 Controller. DSC thermograms, used for activation energy and heat of reaction analysis, were obtained for the various formulations using heating rates of 2.5, 5.0, 10.0, and 20.0°C per minute. Sample sizes were maintained at approximately 15 mg. Subambient DMA was used to investigate the glass transition temperature(s) of the cured systems. A heating rate of 5°C per minute was used with a test frequency of 1.0 Hz and an oscillation amplitude of 0.2 mm.

Various mechanical tests were utilized to characterize the model adhesive's performance. These tests included single lap shear and both mode I (double cantilever beam) and mode II (end-notch flexure) fracture toughness. The adherends used in all cases were woven carbon fiber epoxy prepreg material. Single lap shear specimens were prepared with precured composite panels (177°C) which were sanded and solvent-wiped prior to final fabrication. A cure cycle with heat-up and cooling rates of 2.77°C per minute was used with a two-hour 177°C hold temperature under vacuum pressure. Channels were machined into the composite adherends to give lap dimensions of approximately 6.45 $cm^2$ (1.0 $in.^2$). Five samples were tested for each resin system using a Universal Testing Machine (Instron 4505) with a crosshead speed of 1.27 mm (0.05 in.) per minute until failure was realized.

Mode I and II fracture toughness specimens were also fabricated using carbon fiber composite panels. Eighteen plies of prepreg were used with a midplane layer of the adhesive in interest to give a final cured thickness of 4.06 mm (0.16 in.). Two minutes compaction time under vacuum was performed before the addition of the next layer of prepreg or adhesive was allowed. A fluorinated ethylene propylene (FEP) copolymer film was placed in the midplane layer to act as a crack starter. Unlike the single lap shear samples, however, the prepreg and adhesive materials were cocured for this situation. A cure cycle identical to the one listed previously was utilized, except that the compaction pressure was increased to 172 kPa (25 psi). Sample dimensions prior to testing were approximately 33.0 $\times$ 1.27 $\times$ 0.41 cm (13 $\times$ 0.5 $\times$ 0.16 in.). Both fracture test methods were performed with a Universal Testing Machine.

Double cantilever beam (DCB) specimens were tested to determine mode I fracture toughness[21,22] using a crosshead speed of 2.54 cm (1.0 in.) per minute until a final displacement of 6.35 cm (2.5 in.) was encountered. The energy required to propagate the resulting crack was recorded, along with the sample width and crack length. Five samples were tested for each adhesive, with each sample yielding one mode I toughness value.

End-notch flexure (ENF) samples were also tested in the Instron using a crosshead speed of 0.254 cm (0.1 in.) per minute to yield mode II fracture toughness values.[21,22] The crack tip was positioned using a 2.5$\times$ magnifying apparatus to 1 in. from both the support and loading pin. The sample was loaded until crack propagation (unstable) occurred. The same sample was then repositioned so the crack tip was once again at the required setting. One sample was tested for each adhesive, from which five to six different mode II values were collected and averaged.

Lastly, optical microscopy was used to investigate the morphological aspects of the various resin systems. An imaging analysis software program was used to calculate representative dispersed phase volume fractions from the micrographs.[23] This was accomplished using a binary imaging contrasting technique and recording characteristic pixel values.

## RESULTS AND DISCUSSION

As previously mentioned, the original raw materials used in each of the model adhesive systems were identical. A ratio of the epoxies was chosen as to provide a balance between inherent brittleness, which reduces adhesive properties, and tack, which can affect void formation during cure as a result of entrapped air.[24] As mentioned, BPA was used as a chain extender in the formulations to increase the molecular weight between crosslinks. Bisphenol A has also been found to increase various end-use properties when used in this capacity.[6,7] It is thought that BPA increases the fracture toughness values by forming a bimodal particle distribution within the resin system. After the base components were chosen, the total equivalent content of the epoxide groups was found, and the amount of curing agent and accelerator were set accordingly. A ratio of 2.5 for the curing agent to accelerator weight was chosen such that their total reactive equivalent contribution equaled 80% of that calculated for the epoxy, BPA, and reactive rubber mixture. This was done to account for nonideal conversions of the epoxide groups, as well as the complex reaction functionality concerning dicyandiamide.[25,26] This level has been shown to be reasonable for similar material systems.[27]

The formulating procedures used to prepare the model resins, however, were changed between each model adhesive system. The different formulating procedures are schematically summarized in Figure 1. For example, resin D was prepared by prereacting the difunctional epoxy with the bisphenol A and separately prereacting the reactive rubber with the tetrafunctional epoxy. After the different prereactions were completed, the two mixtures were combined, and the curing agent

and accelerator incorporated. Other permutations were not chosen because the formulations were not practical from a fabrication aspect (i.e., semisolid formation at 145°C). An untoughened sample was also created for dynamic mechanical analysis by reacting the difunctional epoxy with the bisphenol A and then adding the tetrafunctional epoxy and curing agent–accelerator mixture.

## Mechanical Testing

The results of the single lap shear specimens for the model systems are shown in Figure 2. These samples were prepared with precured carbon fiber–epoxy prepreg material, and final bond thicknesses were consistent between samples at approximately 0.14–0.20 mm. The various samples had similar void contents in the final cured materials (slightly more than the commercial system analyzed). This was due to a slightly higher tack value associated with the model systems. This increased tack resulted in an increase in entrapped

Part A

- Epon ® 828
- Araldite ® MY9512
- Hycar ® 1300x9 CTBN
- Bisphenol A

Part B

Epon ® 828
Diuron
Dicy

Model Formulating Procedure

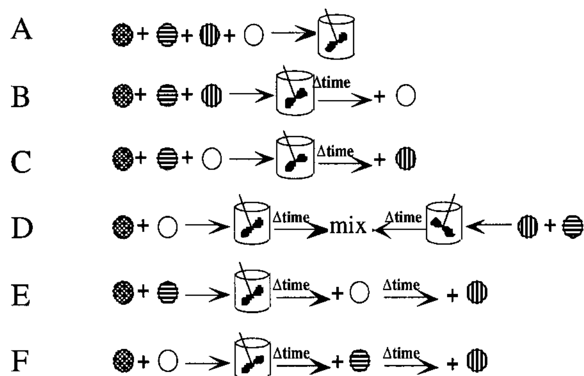


**Figure 1** Formulating procedures used for different model system development.

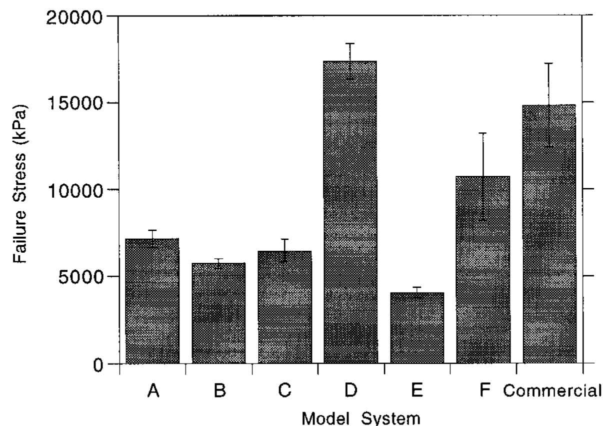


**Figure 2** Single lap shear values for model adhesive systems with precured carbon fiber composite adherends.

air that remained during cure. Also shown in the figure is the lap shear result for a currently used commercial aerospace adhesive film. The results show quite clearly that the formulating dependency was significant and that model system D was the only model system that performed as well or better than the commercial system. This was supported by the fact that system D was the only model to show cohesive failure during the testing. All other samples showed adhesive failure during the single lap shear tests (except for the commercial system). These results indicated that the formulating procedure affected the bonding ability of the adhesive to the precured panel during cure. Therefore, the adhesive capability, being a complex function of flow, wetting, secondary bonding interactions, etc., can be manipulated by the way the materials are prereacted before the final cure cycle.

Fracture toughness tests, used frequently to characterize toughened resin systems, were performed on the model adhesive systems using the same prepreg material as the single lap shear specimens. However, the samples for the fracture tests were cocured instead of bonded (precured). Both mode I and II fracture specimens were prepared and tested. The relationships used for the fracture toughness calculations are represented by

$$\text{Mode I:} \quad G_{\mathrm{Ic}} = \frac{\Delta E}{\Delta a \cdot w} \tag{1}$$

$$\text{Mode II:} \quad G_{\mathrm{IIc}} = \frac{9P_c \cdot C \cdot a^2}{2w[2l^3 + 3a^3]} \tag{2}$$

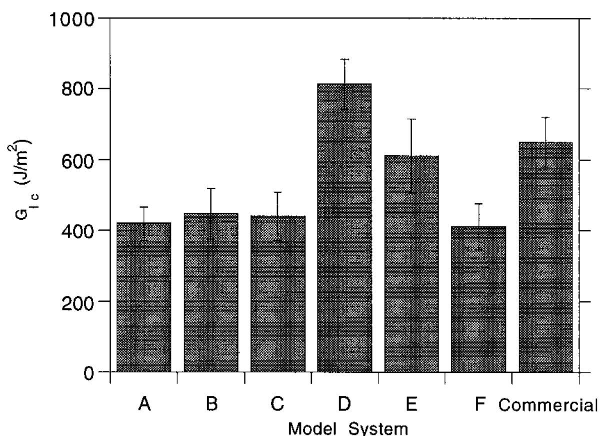


**Figure 3** Mode I (DCB) fracture toughness values for model adhesives cocured with carbon fiber composite adherends.

where $\Delta E$ denotes the energy released in crack growth, $a$ is the crack length, $w$ is the sample width, $P_c$ is the maximum load, $C$ is the material compliance, and $l$ is the length to the loading point.[21,22] The results of the fracture tests appear in Figures 3 and 4. All samples for fracture testing were void-free at the bondline interface and in the bulk of the adhesive. This is important since fracture toughness values can be affected considerably by the presence of voids within the toughening material or at the interface.[22]

The fracture results followed the trend observed for the lap shear results. For the mode I or opening fracture tests, model system D again outperformed the other model samples, as well as the commercial system. Model D was also, again, the only model to have cohesive failure during the testing process. This, again, reinforced the idea that bonding and/or interactions between the two resin systems during cure were not being formed in the other model systems to the degree that they were in model D.

The mode II fracture results were slightly different from those observed for the mode I testing. Mode II analysis indicated that system $F$ was the toughest of the model systems in the shear loading and fracture mode. The three toughest adhesives in mode II all had cohesive failure, while only the two toughest in both mode I and lap shear showed this type of failure. Mode II information suggested that in-plane shear fracture might be more prone to failure in the bulk adhesive material versus crack jumping between the interface and bulk material. This would seem to contradict the earlier results where interfacial or adhesive failure was prominent for the specimens; however, it is probable that the lap shear specimens were subjected to some small but finite peel stresses at the edges of the laps during testing. Assuming this point to be where crack initiation started prior to failure (values of $G_{IIc}$ much larger than $G_{Ic}$), the crack would tend to propagate or rupture at the interface during failure if the mode I toughness was not great enough. Therefore, single lap shear trends should seem to closer approximate fracture mode I values, as was observed. The reason why model F possessed an increased mode II fracture toughness may be related to the adhesive layer thickness. Mode F had a bond thickness approximately 20% thicker than the other systems. This increased bond thickness can lead to an increase in fracture toughness, provided the deformation zone was of the order of the bond thickness.[10,13,28–30] The increased thickness would allow for a larger plastic deformation zone, resulting in a greater fracture toughness value observed.

## Optical Microscopy

To further support the previous hypotheses, optical micrographs were taken of the lap shear specimens, as well as the fracture samples, to investigate the morphology. The dispersed phase in the models was clearly visible without the need for enhancing techniques (e.g., staining). The commercial system, however, had particles that were masked by pigment or too small to be seen with optical microscopy. This was probably a result of the rubber type utilized in the formulations, which would influence the rubber domain size created during cure. The results for the different

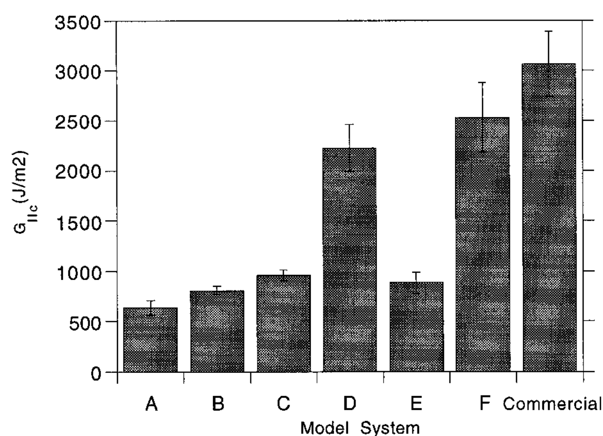


**Figure 4** Mode II (ENF) fracture toughness values for model adhesive systems cocured with carbon fiber composite adherends.

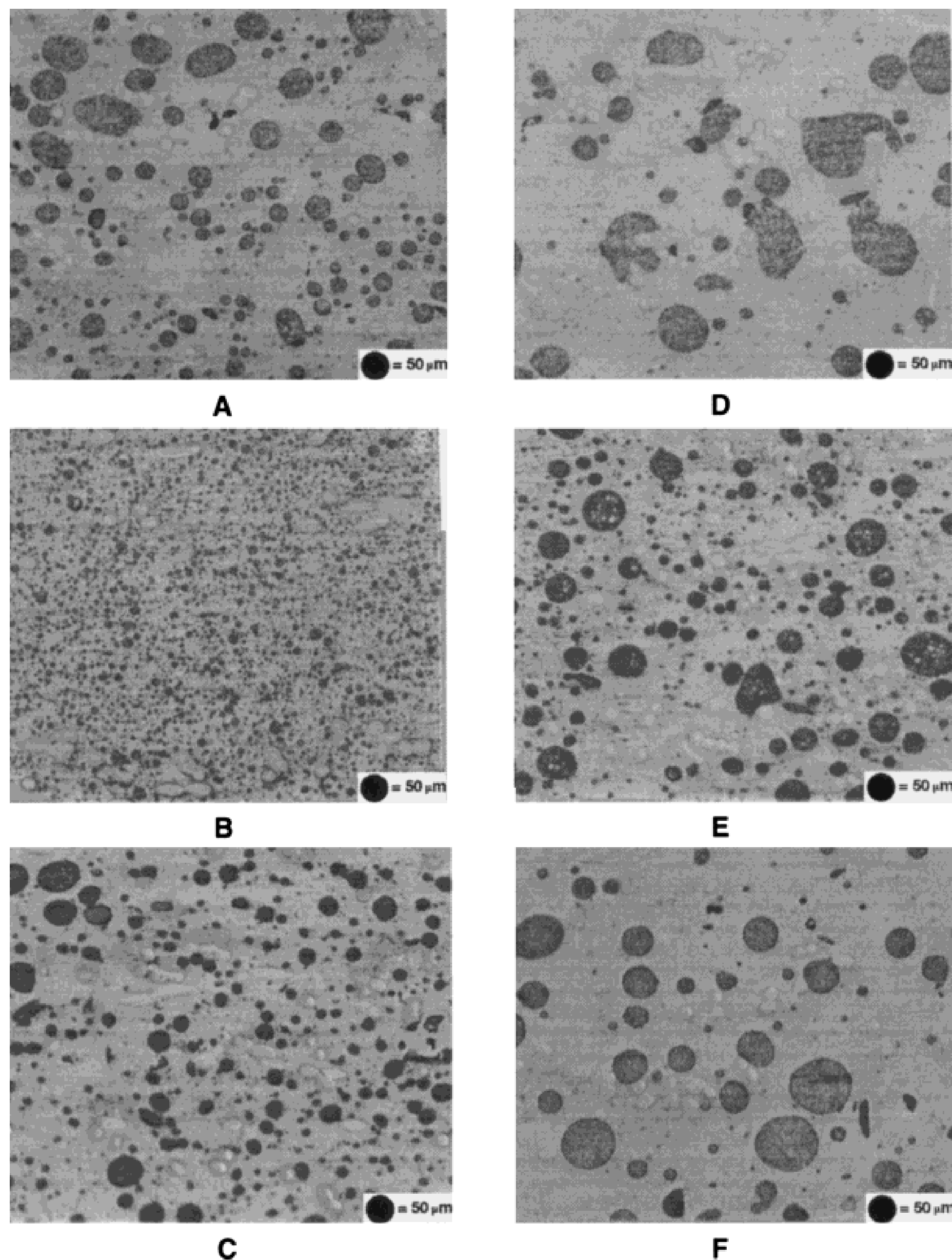


**Figure 5** Optical micrographs of the model epoxy adhesive systems taken at ×200 magnification.

model morphologies are shown in Figure 5. Again, it should be mentioned that all samples were prepared using the same cure cycle and parameters. These micrographs clearly illustrate the differences that can be realized by changing the formulating procedure. A wide range of particle sizes was observed varying from approximately 1.0 to 100 $\mu$m. Also, some particles appeared spherical in shape, while others possessed a more elliptical or nonspherical structure indicative of chain mobility and viscosity constraints during cure. There appeared to be a strong dependence between the formulating procedure and the dispersed phase particle size distribution after cure. Model B displayed a relatively uniform particle size distribution, while models D and F possessed a more bimodal size distribution with particles on the order of 50–75 $\mu$m and another grouping around 1 $\mu$m.

**Table II Dispersed Phase Volume Fractions for Model Adhesive Systems as Determined by Image Analysis**

| Model Adhesive | Volume Fraction Dispersed Phase |
|---|---|
| A | 0.22 |
| B | 0.23 |
| C | 0.20 |
| D | 0.20 |
| E | 0.22 |
| F | 0.18 |

Using image analysis,[23] the volume fraction of the dispersed phase was calculated. Multiple areas were tested for each adhesive to obtain an average value for the volume fraction of the dispersed phase. The results obtained from the imaging analysis appear in Table II. As is evident from the table, the dispersed phase volume fraction seemed to deviate only slightly among the various models. There appeared to be limited formulating dependence on the amount of rubber that phase separated but a strong dependence on the size and distribution of the rubber-rich particles. This behavior is probably a result of the type of reactive rubber used in the models, which has a relatively low solubility parameter (increased butadiene content), promoting more complete phase separation from the epoxy during cure.

### Differential Scanning Calorimetry

In order to help explain the reasons for the results obtained in the mechanical, fracture, and morphological experiments, different thermal analysis techniques were utilized to characterize the model systems. The techniques used included DSC and DMA.

DSC was used to calculate the heat of reaction and apparent activation energy for each of the model systems. The activation energy calculations were based on an Arrhenius temperature dependence for the rate constant and approximations developed by Ozawa[31] and Doyle.[32] The main assumption involved in this analysis is that the extent of reaction at the peak exotherm is constant and independent of the heating rate, which is reasonable for the model epoxy systems used. The equation relating the activation energy to peak temperature and heating rate is given by

$$E_A \approx \frac{-R}{1.052} \cdot \frac{\Delta \ln \phi}{\Delta(1/T_p)} \quad (3)$$

where $E_a$ is the apparent activation energy, $R$ the universal gas constant, $\phi$ the heating rate, and $T_p$ the exotherm peak temperature. The results of the kinetic analysis appear in Table 3.

The calorimetric results for the model adhesive systems suggested that there was not much difference between the model systems' activation energy values, indicative of the same reactions taking place during cure for all of the different model systems. This would be expected since all models had epoxide groups that reacted with the dicyandiamide and diuron during cure (assuming all rubber carboxyl end-groups had been prereacted). Any deviation in the activation energies would imply that some impurities had entered the system, causing undesirable side reactions. It is also possible that deviations could be due to incomplete prereaction steps, but this is unlikely since previous titration tests showed that the time allowed for these steps was sufficient for the temperature and catalyst used in the study. The activation energy determined for the commercial epoxy adhesive system was slightly higher, suggesting that different kinds and/or amounts of curing agent and accelerator were used for the formulation.

The heat of reaction values for the model systems were fairly constant with the exception of system E, whose value fell approximately 20% below the others' average of 290 J/g. Since the other formulations' $\Delta H_{rxn}$ values were consistent and had the same activation energy, one would expect that the number and types of bonds that formed during the curing process were consistent. It appeared, however, that model E had a small reduction in the number of bonds that were created during the curing process. This may be due to any of several different phenomenon, including steric hindrance effects, which reduce reactive site ac-

**Table III Kinetic and Reaction Information for Adhesive Systems as Determined by Differential Scanning Calorimetry**

| Adhesive | $\Delta H_{rxn}$ (J/g) | Activation Energy (kJ/mol) |
|---|---|---|
| A | 275 | 81 |
| B | 306 | 81 |
| C | 273 | 84 |
| D | 297 | 81 |
| E | 245 | 81 |
| F | 277 | 81 |
| Commercial | 309 | 86 |

**Table IV Glass Transition Temperatures for the Adhesive Systems as Determined by the Peak in the Tan δ Signal from Dynamic Mechanical Analysis**

| Adhesive | Low Temperature Peak (°C) | High Temperature Peak (°C) |
|---|---|---|
| Untoughened | −55 | 177 |
| A | −28 | 159 |
| B | −31 | 161 |
| C | −29 | 161 |
| D | −21 | 157 |
| E | −27 | 147 |
| F | −28 | 159 |

cessibility. This effect would result in the formation of fewer hydroxyl groups during cure, which contribute in the secondary bonding aspects between the adhesive and substrate. The lower crosslink density, though, would help improve the fracture toughness values because of the increased ductility of the matrix.

## Dynamic Mechanical Analysis

To further investigate the thermal analytical behavior of the model systems, DMA was used to analyze the phase composition by determining the respective glass transition temperatures. Because of the two phases present, one would expect two distinct transition temperatures evident from the DMA response. This was indeed observed for all of the model systems. There was a subambient temperature transition characteristic of the rubber-rich domains and a higher temperature transition representative of the continuous phase epoxy-rich region. A low-temperature broad transition was also observed for the unmodified (untoughened) adhesive sample which somewhat overlapped with the low temperature response of the toughened systems. This $\beta$ transition is characteristic of the [$-CH_2CH(OH)CH_2O-$] segment in the epoxy component of the resin.[1] The results for the glass transition temperatures of the different systems appear in Table IV.

To analyze the glass transition temperatures of the epoxy-rich (phase 1) and rubber-rich (phase 2) phases obtained from DMA, several methods have been proposed. The two most commonly used procedures involve the Fox equation[33] or the Gordon–Taylor equation.[34] These relationships have been applied for several different modified epoxy combinations with reasonable results.[11,14,35,36] For the analysis in this study, the Gordon–Taylor relationship was chosen because it has shown slightly better agreement with experimental results for flexibilized blends (versus plasticized blends).[35] The CTBN used in the present study was prereacted with the epoxy so that the continuous phase was flexibilized rather than plasticized. In any case, both methods of analyzing the dynamic mechanical data result in similar trends; only the magnitudes of the calculated values differ slightly. The Gordon–Taylor relationship relates the change in glass transition temperature $\Delta T_{g,E}(T_{g,E(0)} - T_{g,E(r)})$ of the epoxy-rich phase to the mass fraction of rubber ($w_r^c$) in this phase such that

$$\Delta T_{g,E} = \frac{k w_R^c (T_{g,E(0)} - T_{g,R(0)})}{1 + w_R^c (k - 1)} \qquad (4)$$

where $T_{g,E(r)}$ is the observed glass transition temperature for the epoxy-rich phase, $T_{g,E(0)}$ and $T_{g,R(0)}$ are the glass transition temperatures of the neat epoxy (cured) and rubber, and $k$ is a theoretical parameter related to the thermal expansion jump of the materials at the glass transition. The value of $k$ can be estimated from data available in literature or directly calculated from eq. (4) if total dissolution is observed. The $k$ value can be represented using the relationship

$$k = \frac{\Delta\alpha_E / \rho_{E(T=T_g)}}{\Delta\alpha_R / \rho_{R(T=T_g)}} \qquad (5)$$

where $\Delta\alpha$ is the change in thermal expansion coefficient at the glass transition, and $\rho$ is the density at this point. Assuming that both the epoxy and rubber components follow the Simha–Boyer relationship[37] given by

$$\Delta\alpha_i \cdot T_{g,i} \cong 0.113 \qquad (6)$$

$k$ can be estimated as

$$k = \frac{\rho_E T_{g,E(0)}}{\rho_R T_{g,R(0)}} \qquad (7)$$

For the present study, the $k$ value calculated using eq. (7) was 2.44.

The volume fraction of rubber in the continuous phase can be calculated with

**Table V Butadiene–Acrylonitrile Rubber–Toughener Content for the Different Phases of the Model Adhesive Systems**

| Model Adhesive | Volume Fraction Phase 1 | Volume Fraction Phase 2 |
|---|---|---|
| A | 0.036 | 0.46 |
| B | 0.031 | 0.46 |
| C | 0.031 | 0.52 |
| D | 0.041 | 0.49 |
| E | 0.065 | 0.36 |
| F | 0.036 | 0.56 |

$$\Phi_{R,1} = \frac{w^c_{R,1}/\rho_R}{w^c_{R,1}/\rho_R + w^c_{E,1}/\rho_E} \quad (8)$$

where $\Phi_{R,1}$ the mass fraction of rubber in phase 1, and $\rho_R$ and $\rho_E$ are the densities of the pure rubber and neat epoxy. The density values used in the analysis were $\rho_R = 0.955$ g cm$^3$ and $\rho_E = 1.15$ g cm$^3$. After using image analysis to determine the volume fraction of the dispersed phase, the rubber-rich phase composition was calculated using a mass balance to give

$$\Phi_{R,0} = (1 - V_D)\cdot\Phi_{R,1} + V_D\cdot\Phi_{R,2} \quad (9)$$

where $V_D$ is the volume fraction of the dispersed phase. The results of the compositional analysis are shown in Table V.

The epoxy-rich phase compositional values were fairly consistent at around 3–4 vol % rubber, except for model system $E$. The volume percentage of dissolved rubber in system $E$ was almost doubled in comparison to the other systems, suggesting that the formulating procedure influenced the phase separation behavior by limiting the dispersed phase formation during the cure process. This increased dissolved rubber in the continuous phase may result in decreased bonding between the adhesive and substrate materials by limiting the polar interactions between substrate and adhesive. Decreased mechanical properties, particularly adhesive failure, were observed for system $E$, suggesting that this scenario may be possible. The amount of flexibilized rubber alone, however, cannot sufficiently explain the mechanical behavior observed by the model systems. System $D$ had slightly more rubber in the continuous phase than the other systems (excluding $E$) but still possessed superior performance characteristics.

To further help understand the material performance values, the volume fraction, size, and shape of the dispersed domains must be considered. Except for sample $E$, all models had approximately the same dispersed phase composition, regardless of size and shape of the domains. This is supported by systems $B$ and $D$ or $F$, which have vastly different morphological characteristics, as far as dispersed phase size is concerned, but nearly equal compositions. The polymer mobility and structure prior to gelation when the secondary phase is created during cure then becomes an important issue. Some of these mobility issues were evident in the DSC thermal analysis results by changes in the total heats of reaction. The more mobile systems would be expected to display larger dispersed domains (assuming the same composition in these phases). This increased mobility could result in a less stressed region, both in the bulk and interfacial regions, after cure and cool down, which would result in better performance values. However, these large rubber particles are not always desirable since toughening is optimized with a secondary phase on the order of 0.1–5 $\mu$m.[4] Samples $D$ and $F$ were the only samples with regular particles on the order of 1 $\mu$m, explaining some of the reason why these materials behaved well in fracture testing. Therefore, for this particular rubber modifier, increased mobility may lead to less stressed final parts, but at an increase of the dispersed phase size. This provides a trade-off between adhesive performance (bonding ability to substrate) and maximized fracture characteristics, which needs to be addressed for different systems in question.

From this study, it was concluded that the formulating procedure does play a role in the final material morphology and performance of rubber toughened epoxies. Alterations in these procedures influenced the size and shape of the dispersed domains as well as the composition of the continuous phase. The amount of rubber flexibilizing the system in the continuous phase, as well as the mobility of the system during cure, in turn affected the properties that were observed for the final cured parts.

## CONCLUSIONS

A study was conducted investigating the influence of formulating procedure on the morphology and performance of adhesive materials. Model epoxy adhesive systems were created using a CTBN reactive rubber modifier for increased toughness

characteristics. Material analysis included DSC, DMA, lap shear testing with precured composite panels, mode I and II fracture testing with cocured composite panels, and optical microscopy.

The formulating procedure was found to have a strong influence on the mechanical and fracture properties, indicating that specific prereactions involving the initial material components can significantly affect part quality. DSC revealed that the activation energies for the different model systems remained unchanged; but the total heat of reaction was affected, showing that some reactive sites did not participate in the curing reaction. DMA was used with the Gordon–Taylor analysis method to estimate the composition of the continuous epoxy-rich phase. The analysis suggested that increased flexibilized rubber content in the continuous phase may have hindered slightly the adhesive ability of the model systems during cure. This analysis also demonstrated that, for the most part, regardless of dispersed phase size and shape, the composition of the dispersed phases remained the same.

Optical microscopy showed that the morphology was strongly affected by the formulating procedure. A wide range of particle sizes was observed for the different model systems. The superior model adhesive systems appeared to possess a bimodal distribution with particles on the order of 1 and 50 $\mu$m. The larger diameter particles indicated that increased mobility of the polymer segments during cure may lead to final parts with less residual stresses, resulting in the advanced performance values observed.

The authors wish to express their thanks to The Boeing Co., TA Instruments, and Sovereign Engineered Adhesives for their continued support through the Polymeric Composites Laboratory consortium at the University of Washington.

## REFERENCES

1. C. A. May, *Epoxy Resins,* Marcel Dekker, New York, 1988.
2. C. B. Bucknall and T. Yoshii, *Brit. Polym. J.,* **10,** 53 (1978).
3. H. Hsich, *Polym. Eng. Sci.,* **30,** 493 (1990).
4. A. J. Kinloch, S. J. Shaw, D. A. Tod, and D. L. Hunston, *Polymer,* **24,** 1341 (1983).
5. W. N. Kim, C. E. Park, and C. M. Burns, *J. Appl. Polym. Sci.,* **50,** 1951 (1993).
6. I. K. Partridge and G. M. Maistros, *Plastics, Rubber Comp. Proc. and Applications,* **23,** 325 (1995).
7. C. K. Riew, E. H. Rowe, and A. R. Siebert, in *Toughness and Brittleness of Plastics; Advances in Chemistry 154,* R. D. Deanin and A. M. Crugnola, Eds., American Chemical Society, Washington, DC, 1976.
8. A. R. Siebert, L. L. Tolle, and R. S. Drake, *Adhes. Age,* **29,** 19 (1986).
9. W. A. Romanchick, J. E. Sohn, and J. F. Geibel, in *Epoxy Resin Chemistry II,* R. S. Bauer and M. J. Comstock, Eds., ACS Symposium Series, American Chemical Society, Washington, DC, 1983.
10. H. Chai, *Acta Metall. Material.,* **43,** 163 (1995).
11. L. C. Chan, J. K. Gillham, A. J. Kinloch, and S. J. Shaw, in *Rubber-Modified Thermoset Resins,* C. K. Riew and J. K. Gillham, Eds., American Chemical Society, Washington, DC, 1984.
12. A. J. Kinloch, in *Rubber-Toughened Plastics; Advances in Chemistry,* C. K. Riew, Ed., American Chemical Society, Washington, DC, 1995.
13. N. Sela, O. Ishai, and L. Banks-Solls, *Composites,* **20,** 257 (1989).
14. D. Verchére, H. Sautereau, J. P. Pascault, S. M. Moschair, C. C. Riccardi, and R. J. J. Williams, in *Toughened Plastics I: Science and Engineering; Advances in Chemistry Series,* C. K. Riew and A. J. Kinloch, Eds., American Chemical Society, Washington, DC, 1993.
15. K. Yamanaka and T. Inoue, *J. Mater. Sci.,* **25,** 241 (1990).
16. J. C. Seferis, *SAMPE J.,* **24,** 6 (1988).
17. W. J. Lee, J. C. Seferis, and D. C. Bonner, *SAMPE Quart.,* **17,** 58 (1986).
18. M. A. Hoisington and J. C. Seferis, *SAMPE Quart.,* **24,** 10 (1993).
19. K. Didden, R. Grove, S.-H. Kim, R. McCullough, B. Roundtree, S.-B. Shim, B. Hayes, K.-J. Kim, C. Martin, L. Nguyen, T. Pelton, J. Putnam, D. Renn, C. Watson, Y. T. Shim, and J. S. Seferis, *Staged Protocol for Global Technology Implementation: Composites with Dual Cure for Manufacturing and Repair,* University of Washington, Seattle, 1996.
20. M. A. Hoisington, D. Thompson, and J. C. Seferis, in *Proceedings of 37th International SAMPE Symposium,* SAMPE, Anaheim, 1992, p. 264.
21. N. J. Pagano, *Interlaminar Response of Composite Materials,* Elsevier, New York, 1989.
22. J. W. Putnam, Ph.D. thesis, University of Washington, 1996.
23. W. Rasband, *Void Analysis Was Performed on a Model 7100 / 80 Power MacIntosh Using the Public Domain NIH Image Program* (available from the Internet by anonymous ftp from zippy.nimh.nih.gov or on floppy disk from NTIS, 5285 Port Royal Rd., Springfield, VA 22161, part no. PB93-504868).
24. B. S. Hayes, to appear.
25. M. D. Gilbert, N. S. Schneider, and W. J. MacKnight, *Macromolecules,* **24,** 360–369 (1991).

26. T. Guthner and B. Hammer, *J. Appl. Polym. Sci.,* **50,** 1453 (1993).
27. B. H. Hayes and J. C. Seferis, in *Proceedings of the 28th International SAMPE Technical Conference,* SAMPE, Seattle, 1996.
28. A. J. Kinloch, *Adhesion and Adhesives: Science and Technology,* Chapman and Hall, New York, 1987.
29. D. L. Hunston, A. J. Kinloch, and S. S. Wang, *J. Adhes.,* **28,** 103 (1989).
30. W. D. Bascom, in *Adhesion,* K. W. Allen, Ed., Applied Science, New Jersey, 1982.
31. T. Ozawa, *J. Therm. Anal.,* **2,** 301 (1970).
32. C. D. Doyle, *J. Appl. Polym. Sci.,* **5,** 285 (1961).
33. T. G. Fox, *Bull. Am. Phys. Soc.,* **1,** 123 (1956).
34. M. Gordon and J. S. Taylor, *J. Appl. Chem.,* **2,** 493 (1952).
35. P. Bussi and H. Ishida, *Polymer,* **35,** 956 (1994).
36. D. Chen, J. P. Pascault, H. Sautereau, R. Ruseckaite, and R. J. J. Williams, *Polym. Int.,* **33,** 253 (1994).
37. R. Simha and R. F. Boyer, *J. Chem. Phys.,* **37,** 1003 (1962).